

Chapter 2: Population genetic structure in a metapopulation of a coral reef fish: asymmetric migration rates and scale-dependency.

Publication: Bay LK, Caley MJ and Crozier RH (In Review) Population genetic structure in a metapopulation of a coral reef fish: asymmetric migration rates and scale-dependency. *Molecular Ecology*

Abstract

Using mtDNA control region sequences ($n = 283$) and three microsatellite loci ($n = 316$), I examined the the spatial genetic structure on the Great Barrier Reef, Australia, of a direct developing coral reef fish, *Acanthochromis polyacanthus*, with comparatively low dispersal rates. I employed a hierarchical sampling design to test three models of genetic structuring (i.e., the island, isolation-by-distance and metapopulation model) at multiple geographical scales (among regions ($n = 3$), among continental shelf positions within regions ($n = 3$), and among reefs within regions ($n = 5 - 6$)). I also tested for asymmetric migration rates among locations using multiple molecular markers. The spatial genetic structure of this species was scale-dependent. Significant genetic structure ($\Phi_{ST} = 0.81$, $R_{ST} = 0.2$, $F_{ST} = 0.07$, $P < 0.0001$) and evidence of isolation-by-distance (Φ_{ST} vs. km $r = 0.77$, $P = 0.001$, R_{ST} vs. km $r = 0.53$, $P = 0.002$, F_{ST} vs. km $r = 0.46$, $P = 0.001$) was found among regions. Within regions, significant structuring across the continental shelf was evident in some regions (North: $\Phi_{ST} = 0.31$, $P < 0.001$; Central: $R_{ST} = 0.11$, $P = 0.015$) but no evidence of isolation-by-distance was present at this spatial scale ($P > 0.05$ in all cases). Very strong genetic structure was detected among reefs within regions (mean fixation within region: $\Phi_{ST} = 0.28 - 0.41$, $R_{ST} = 0.09 - 0.13$, $F_{ST} = 0.06 - 0.1$) suggesting that *A. polyacanthus* displays metapopulation dynamics at this scale. Pairwise genetic distances increased from offshore and older populations, to inshore and younger ones, in all comparisons that included significant fixation indices. These patterns support a metapopulation propagule-pool model of colonisation. Based on mtDNA, reciprocal migration rates were low and asymmetric, but based on microsatellites high and symmetrical. These contrasting patterns suggest that the genetic structure observed here may be influenced by male-biased dispersal.

Introduction

The evolution of spatial genetic structure in animal and plant populations has been a central focus of evolutionary studies, and has been important in the development of metapopulation theory. This theory is intended to understand systems of ephemeral, genetically subdivided populations that persist through time via colonisation and migration from source populations (Hanski 1991; Hanski and Gilpin 1997; Pannell and Charlesworth 2000). Such populations are characterised by having a level of migration that is high enough to recolonise extinct populations, but low enough for drift to generate measurable genetic differences among populations (Hanski and Gilpin 1997). While earlier models assumed that migration was infrequent, occurring only to recolonise patches that had gone extinct (Levins 1970; Slatkin 1977), it is becoming evident that in metapopulations, migration rates may be asymmetric (Stacey et al. 1997) and vary temporally (e.g., Harrison 1991; Stacey and Taper 1992) and spatially (e.g., Pulliam 1988; Hanski and Gyllenberg 1993; Valone and Brown 1995). Behavioural differences among individuals (e.g., Aars and Ims 2000; Blundell et al. 2002; Fraser et al. 2004) can further contribute to such variation. In turn, such variation in migration rates should generate a diversity of genetic signatures depending on the relative importance of each process contributing to its generation (Pannell and Charlesworth 2000). Analytical techniques that can separate overall genetic differentiation into reciprocal migration rates (Beerli and Felsenstein 1999, 2001) should, therefore, be able to illuminate the roles of various processes in establishing patterns of genetic differentiation among sub-populations.

Models of the genetic structure of populations have developed from Wright's original island model (Wright 1931) to the stepping-stone, or isolation-by-distance models, by incorporating spatial variation (Wright 1943; Kimura 1955; Kimura and Weiss 1964; Weiss and Kimura 1964), and later to metapopulation models which incorporate differences in effective population sizes, colonisation and extinction rates (e.g., Slatkin 1977, 1985, 1987; Wade and McCauley 1988; Whitlock and McCauley 1990). Theory suggests that the sources and rates of colonisation relative to subsequent migration are critical determinants of the evolution of genetic structure of a metapopulation (Wade and McCauley 1988; Whitlock and McCauley 1990; Pannell and Charlesworth 2000). In a metapopulation with low levels of migration, the metapopulation propagule-pool model predicts high genetic differentiation if empty patches are colonised by individuals from a single source (Wade and McCauley 1988;

Whitlock and McCauley 1990). In contrast, under the metapopulation migrant-pool model, low genetic differentiation may occur if individual patches are colonised by migrants from a range of sources (Wade and McCauley 1988; Whitlock and McCauley 1990). Under the propagule-pool model, genetic differentiation will always be greater than under an island model. Under a migrant-pool model, a metapopulation should have greater genetic differentiation among populations compared to an island model if colonisation and migration rates are similar (e.g., $4N_e m = 2k$, $4N_e m$ = effective number of migrants, k = number of colonisers) (Wade and McCauley 1988; Whitlock and McCauley 1990). Despite recent developments in the theory of structured populations, the genetic consequences of metapopulation dynamics remain unclear (Olivieri et al. 1990; Gilpin 1991; McCauley 1991; Harrison and Hastings 1996) due, to a considerable extent, to a lack of empirical tests.

Separating the effects of colonisation pattern and subsequent migration in metapopulations is often difficult because the relative effects of colonisation and migration cannot be estimated from a single estimate of genetic differentiation (Giles and Goudet 1997). However, if the conditions of the propagule-pool model hold, or if colonisation and migration is the same process, then younger populations should display greater genetic differentiation compared to older ones (Giles and Goudet 1997; Pannell and Charlesworth 2000). Consequently, it should be possible to distinguish different types of metapopulation dynamics by the amount of genetic structure among populations and by the distribution of genetic differentiation among older and younger populations.

Fishes on coral reefs occupy a naturally fragmented environment where patches of suitable reef habitat are surrounded by unsuitable habitat such as open sand and deep water. This physical structure makes coral reefs a good system for studying metapopulation dynamics. At present, however, we know little about the presence, spatial extent and genetic consequences of metapopulations dynamics in marine systems (but see Planes et al. 1996). The vast majority of coral reef fishes have a bipartite life history (Sale et al. 1980; Leis 1991; Leis and Carson-Ewart 2000), where pelagic larvae have the potential to disperse widely (Doherty et al. 1995; Chapter 5). Associated with this life-history pattern, little genetic structure across relatively large geographical distances is commonly observed (Planes and Fauvelot 2002; Bay et al. 2004; Chapter 5). While such species may be characterised by isolation-by-distance at large spatial scales (e.g., Planes and Fauvelot 2002; Bay et al. 2004) the lack of within-location

sampling by many of these studies make detailed conclusions regarding migration patterns of such species hard to draw. In contrast, species with short, or non-existent larval durations generally display considerable genetic structure across small spatial scales (Bernardi 2000; Planes et al. 2001; Bernardi and Vagelli 2004; Hoffman et al. 2005). While these studies indicate that such species may display metapopulation dynamics, the sampling strategies used have not permitted detailed examinations of this issue.

Species such as *Acanthochromis polyacanthus*, a common fish on the Great Barrier Reef (GBR) which do not have a dispersive larval phase, coupled with the physical history of the GBR, provides an opportunity to examine metapopulation dynamics and the evolution of genetic structure on small spatial scales in a natural marine system. The reefs of the GBR are relatively young (approximately 6000 - 9000 yrs) (Hopley and Thom 1983; Larcombe 2001). Colonisation of these reefs by fishes is likely to have taken place from Pleistocene fringing reefs and offshore refugia (Davies 1989). Based on reef position and present current patterns (Church 1987; Andrews and Clegg 1989), colonisation is likely to have progressed from the outer continental shelf to inner shelf locations. Here I define the age of populations based on reef position and the population expansion times estimated in Chapter 3. Where the variation in the expansion times did not allow the age of populations to be distinguished, I assume for the purposes of this chapter that populations of this species on the outer shelf are older than those at inner shelf locations and hereafter are referred to as older and younger populations. Previous investigations of *A. polyacanthus*, as well as the presence of several colour morphs on the GBR, suggest that sufficient time has elapsed since colonisation began for this species to have evolved genetic differences among populations separated by small geographic distances (Doherty et al. 1994; Planes et al. 2001).

Here I examine the genetic structure of *A. polyacanthus* on the Great Barrier Reef using rapidly evolving mtDNA and microsatellite molecular markers. I examine if and how the genetic structure of this species varies at three spatial scales (i.e., among reefs within continental shelf position, continental shelf position within regions, and among regions) and evaluate spatial and behavioural differences in migration rates. I then examine the evidence for an island, stepping stone or metapopulation model of genetic structure. First, I evaluate if genetic structure follows a stepping stone model by examining the evidence for isolation-by-distance using conventional genetic estimates

of fixation. Next, I evaluate whether the spatial structure of this species follows predictions from the metapopulation propagule-pool and migrant-pool models by evaluating estimates of fixation among older and younger populations. Finally, I examine differences in estimates of genetic differentiation among molecular markers and statistical approaches and discuss potential sources of such variation.

Methods and Materials

Study species and sampling locations

A total of 327 individual *A. polyacanthus* was collected from 15 back-reef locations from 3 regions on the Great Barrier Reef during 2000, 2003 and 2004 (Table 1, Fig. 1) by either spearing with hand-held spears or baited fence netting and hand nets. Baited netting involved aggregating *A. polyacanthus* by baiting the water immediately in front of a 3 x 1.5 meter monofilament net with processed bran, then chasing the fish into the net before catching them with hand held nets. When using this procedure the fence nets were moved regularly to avoid collections of family groups. Fish were transported either alive or on ice to the nearest shore where genetic samples (fin clips) were taken and preserved in 80% EtOH. Genetic structure within regions (shelf effects) were explored independently for two regions (i.e., north and central). Because the southern region contains no true inner and midshelf, the genetic structure in this region was explored using pairwise genetic distances.

DNA extraction and amplification

356 base pairs of the mitochondrial hyper variable control region I were amplified, sequenced in both forward and reverse directions, and aligned in fish from 15 reefs in three regions following methods outlined in Chapter 5. Representative sequences have been deposited in GenBank under accession numbers DQ199666 – DQ199947.

Four microsatellite loci (Miller-Sims et al. 2005) were screened (AC33, AC37, AC42, AC45,) but only 3 loci consistently amplified in both southern, mid and northern populations (AC33, AC37, AC42). Analysis was, therefore, restricted to these loci. Population genetic investigations commonly use a single mitochondrial marker, which introduces some uncertainty about whether results are gene specific or representative of population level processes (Avisé 2000). Therefore, the analysis of microsatellites here was intended to provide an assessment of population structure independent of the

mtDNA. Because of the relatively low number of microsatellite loci screened, interpretations based on these data should be regarded with some caution.

Table 1: Locations, shelf position and geographic coordinates of the 15 populations of *Acanthochromis polyacanthus* sampled in this study. Location abbreviations used throughout this paper are also indicated. Number of alleles sampled: mtDNA = N, microsatellites = 2N.

Region	Shelf	Location	Abbreviation	Latitude; Longitude	Number of alleles sampled	
					mtDNA	Microsatellites
North	Outer	Yonge Reef	YON	14°37S; 145°37E	20	48
		Day Reef	DAY	14°31S; 145°33E	22	44
	Mid	Lizard Island	LIZ	14°40S; 145°28E	20	36
		North Direction	NDR	14°44S; 145°30E	19	48
	Inner	Martin Reef	MAR	14°45S; 145°20E	21	46
		Linnet Reef	LIN	14°47S; 145°21E	20	48
Mid	Outer	Pith Reef	PIT	18°13S; 147°02E	21	42
		Myrmidon Reef	MYR	18°16S; 147°23E	17	46
	Mid	Britomart Reef	BRI	18°14S; 146°39E	19	48
		Trunk Reef	TRU	18°23S; 146°40E	14	30
	Inner	Orpheus Island	ORP	18°37S; 146°29E	21	46
South	Outer	One Tree Island	OTI	23°30S; 152°05E	21	36
	Outer	Sykes Reef	SYK	23°26S; 152°02E	16	62
	Mid	Polmaise Reef	POL	23°34S; 151°41E	13	18
	Outer	Broomefield Reef	BRO	23°16S; 151°57E	19	34

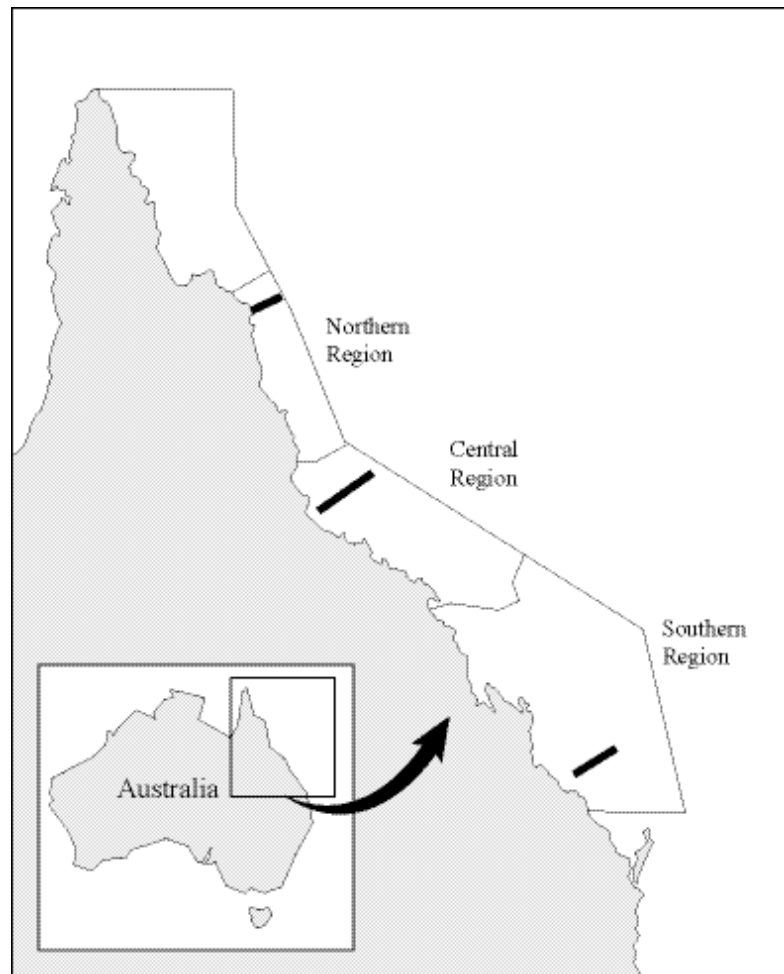


Fig. 1: The sampling locations of *Acanthochromis polyacanthus* on the Great Barrier Reef. Dark bars indicate locations of cross shelf sampling.

The three microsatellite loci were amplified in the same individuals in 15 μ l reactions containing 1x High Fidelity PCR Buffer, 2 mM MgSO₄, 200 μ M each dNTP, 0.4 μ M each primer, approx. 5 ng template DNA and 0.3 units of Hi Fidelity *Taq Polymerase* (Invitrogen Life Technologies). Microsatellites were amplified using a PCR cycling profile of 94 $^{\circ}$ C (5 min), 35 cycles of 94 $^{\circ}$ C (1 min), primer specific annealing temperature (1 min), 68 $^{\circ}$ C (1 min) followed by a final extension phase of 68 $^{\circ}$ C (10 min). Primer specific annealing temperatures were AC37 = 46 $^{\circ}$, AC42 = 52 $^{\circ}$ and AC33 = 46 $^{\circ}$. Fluorolabelled PCR products were cleaned by centrifugation through 300 μ l of sephadex G-50, multiplexed and 0.25 μ l of ET400 standard (Amersham Biosciences) added before genotyping on a Megabase 1000 (Amersham Biosciences) at the Genetic

Analysis Facility in the Advanced Analytical Center, James Cook University. The microsatellite data set is available from the authors upon request.

Data analysis

The mtDNA control region sequences were aligned and edited using Sequencher 4.2 (GeneCodes Corp. Michigan USA) and ESEE (Cabot and Beckenbach 1989). The best model of nucleotide substitution was determined using Modeltest 3.5 (Posada and Crandall 1998) and PAUP* 4.0b10 (Swofford 1998). The hierarchical likelihood tests and Akaike Information Criteria agreed that the Tamura and Nei model (Tamura and Nei 1993) with $\gamma = 0.3012$ fitted the data best (-LogLikelihood = 1220.65; AIC = 2453.30). This model and rate heterogeneity estimate were used in all following analyses of population genetic structure. Base frequencies and the ts/tv ratio from all sampled fish combined were calculated using Modeltest. The role of saturation was explored by comparing the topology of neighbour joining trees (implemented in PAUP*) including and excluding transitions. All individuals retained membership in the same major clades and transitions were included in all further analyses. Linkage among the three microsatellite loci was investigated using Genepop on the Web (Raymond and Rousset 1995). The role of heterozygotic deficit and departure from Hardy-Weinberg equilibrium was investigated using Genalex 6 (Peakall and Smouse 2001) and significance levels were corrected for multiple tests by a sequential Bonferroni correction (Dunn-Sidak method, Sokal and Rohlf 1995). The fit of the Infinite Allele Model (IAM, Kimura and Crow 1963) and the Stepwise Mutation Model (SMM, Kimura and Ohta 1978) was examined using Bottleneck 1.2.02 (Piry et al. 1999).

The mtDNA dataset did not contain any missing data but the microsatellite dataset contained 4% missing values and the majority of these missing values were associated with AC42. To avoid potential confounding effects due to these missing values being treated as a separate allele (Peakall and Smouse 2001), an average genetic identity was allocated to all missing data. This dataset was used in all subsequent analyses of microsatellites.

Population Genetic Structure

Hierarchical population genetic structure of *A. polyacanthus* among regions and reefs was explored using AMOVA using 1000 permutations (Weir and Cockerham 1984; Excoffier et al. 1992) implemented in ARLEQUIN 2.000 (Schneider et al. 2000).

Estimates of population differentiation using microsatellite data were based on both IAM and SMM mutational models. Pairwise genetic distances among populations were calculated from both markers and mutational models using ARLEQUIN and a sequential Bonferroni correction was applied to all pairwise comparisons (Dunn-Sidak method, Sokal and Rohlf 1995).

Migration

Differences in levels of gene flow among locations were investigated further using MIGRATE 1.7.6.1 (Beerli and Felsenstein 1999, 2001). This program calculates reciprocal migration rates (i.e., $4N_e m$ from a to b, and vice versa) using a coalescence maximum likelihood approach (Markov Chain Monte Carlo with Hastings Metropolis importance sampling) and assumes constant mutation rates and equal effective population sizes. Because of the molecular divergences detected by phylogenetic and AMOVA analyses, MIGRATE was run on each geographical region separately and due to different effective population sizes the mtDNA and microsatellite data sets were analysed independently. Reciprocal migration rates were interpreted as significantly different when their 95% confidence intervals did not overlap. Extensive sampling regimes including 10 short chains sampled 10000 times each and 5 long chains sampled 100000 each were averaged over 5 replicate runs. MIGRATE was implemented on a SGI Origin 3800 computer in the James Cook University High Performance Computing Facility. A ts/tv ratio of 1.53 (estimated by Modeltest) was used for the sequence data and a stepwise mutational model was implemented for the microsatellite data. Repeated runs were highly consistent using this sampling strategy. To investigate the potential role of greater sample size of the nuclear marker on estimated patterns of migration, I reduced the microsatellite data sets by one third and one sixth using the same search parameters as above in two ways. First, I randomly removed one third and one sixth of individuals from each location. This resulted in highly inconsistent results among runs for the central and southern regions. Second, I removed two loci and half of the individuals of the remaining locus. This procedure was repeated on all three loci, but only resulted in consistent runs with one locus (AC33), most likely because this locus contained the most information. In the northern region, where the different data reduction strategies could be compared, the results were highly consistent. Therefore, only the reductions to one third and one sixth of individuals of AC33 for all regions are presented below.

Isolation-by-Distance

Isolation-by-distance was explored for both the mtDNA and the microsatellites. Geographical distances among locations were calculated using Vincenty's inverse method (<http://www.ga.gov.au/nmd/geodesy/datums/distance.jsp>). Genetic distances were estimated for mtDNA and microsatellites by conventional genetic distance estimators (Φ_{ST} , F_{ST} , R_{ST}) in ARLEQUIN. Reynold's distance D (Reynolds et al. 1983), Slatkin's linearised measure of similarity (Slatkin and Hudson 1991; Slatkin 1993; Rousset 1997) and Slatkin's measure of M (Slatkin 1995) were also calculated for mtDNA. Microsatellite migration parameters were calculated using IAM ($N_e m$: Hartl and Clark 1997) and SMM ($M = N_e m$: Slatkin 1995) models. Correlation between genetic and geographical distances were tested using a Mantel test (1000 permutations) of both log-transformed and non-transformed data following Smouse et al. (1986) and implemented in Genalex. A sequential Bonferroni correction was used to adjust the significance level of multiple tests (Sokal and Rohlf 1995). Transformations did not affect the overall results. Therefore, only non-transformed km versus Φ_{ST} / F_{ST} / R_{ST} are presented here.

Metapopulation Structure

Predictions from the metapopulation models were tested by comparing estimates of genetic differentiation among older and younger populations in the northern, central and southern regions. In the northern region, variation in the population expansion times (based on mismatch analysis presented in Chapter 3) did not allow older and younger populations to be identified and an age gradient from older outer shelf locations to younger inner shelf locations was examined. In the central region Orpheus Island and Trunk Reef and in the southern region One Tree Island and Sykes Reef were identified as younger (Chapter 3). These locations were compared to older locations (central regions: Myrmidon and Pith Reefs, southern region: Polmaise and Broomefield Reefs).

Results

356 bases of the mtDNA control region I was obtained from a total of 283 individuals collected from 15 reefs. The average base frequencies were AT biased ($A=0.41$, $T=0.40$, $C=0.07$, $G=0.12$) as commonly observed in fish mtDNA (Wolstenholme 1992; McMillan and Palumbi 1997). The ts/tv ratio was 1.53:1 for all samples combined. The

three microsatellites were amplified in 316 individuals. Linkage equilibrium was not rejected for the three microsatellites (AC33 vs. AC37: $\lambda^2 = 37.735$ df = 30 P = 0.157, AC33 vs. AC42: $\lambda^2 = 28.253$ df = 30 P = 0.557, AC37 vs. AC42: $\lambda^2 = 25.871$ df = 30 P = 0.682). Heterozygotes were less abundant than expected according to Hardy-Weinberg expectations in 17 of 45 locus-by-population comparisons (29 of 45 comparisons before Bonferroni correction), however, these departures were not confined to any of the populations or loci in particular (Table 2). Both models of microsatellite evolution were supported: the IAM model was only rejected in 1 and SMM in 6 out of 45 locus-by-population comparisons (Table 2). Significant genetic structure was detected among regions (P < 0.0001) and the strength of fixation differed among molecular markers and mutation models (Table 3). Fixation indices ranged from very high 0.81 (Φ_{ST}), lower 0.2 (R_{ST}) and low 0.07 (F_{ST}) suggesting that the genetic structure among regions differed among the molecular markers used.

For mtDNA, most of the variation occurred among regions (81.2%), whereas, for microsatellites much less variation occurred at this spatial scale (IAM: 7.3 %, SMM: 19.5 %) and more variation was found within populations (IAM: 85.3 %, SMM: 70.3 %) (Table 3). Significant structure could be attributed to shelf position only in the northern region based on mtDNA ($\Phi_{ST} = 0.31$, P < 0.001, c.f. microsatellites: $F_{ST} = 0.04$, P = 0.06, $R_{ST} = 0.04$, P = 0.14). Significant shelf-position effects were evident in the central region based on microsatellites ($R_{ST} = 0.11$ P = 0.015) but not mtDNA ($\Phi_{ST} = 0.097$ P = 0.17) (Table 4).

Table 2: Observed (H_O) and expected (H_E) heterozygosity, probability test of heterozygote deficit (λ^2 (df)), P and Bonferroni corrected significance probability (α), probability of departure from the Infinite Allele Model (IAM) and Stepwise Mutation (SMM) models and their associated Bonferroni corrected significance probabilities (α) of the three microsatellite loci among 15 populations of *Acanthochromis polyacanthus* on the Great Barrier Reef.

Location	Locus	H_O	H_E	Heterozygote excess			IAM		SMM	
				λ^2 (df)	P	α	P	α	P	α
Day Reef	AC37	0.708	0.845	105.8 (78)	0.02	0.002	0.471	0.002	0.051	0.002
	AC42	0.833	0.944	385.7 (325)	0.012	0.002	0.429	0.004	0.250	0.004
	AC33	0.625	0.737	32.94 (21)	0.047	0.003	0.340	0.003	0.208	0.003
Yonge Reef	AC37	0.636	0.753	62.22 (28)	0.000	0.001	0.466	0.02	0.097	0.002
	AC42	0.636	0.777	134.6 (55)	0.000	0.001	0.255	0.03	0.004	0.001
	AC33	0.636	0.755	16.31 (15)	0.362	0.005	0.110	0.05	0.413	0.007
Lizard Island	AC37	0.778	0.764	47.25 (45)	0.381	0.006	0.204	0.002	0.012	0.001
	AC42	0.722	0.944	313.0 (253)	0.006	0.001	0.243	0.002	0.537	0.02
	AC33	0.778	0.776	38.72 (45)	0.734	0.01	0.271	0.002	0.007	0.001
North Direction	AC37	0.542	0.774	130.8 (55)	0.000	0.001	0.249	0.002	0.006	0.001
	AC42	0.625	0.928	263.3 (190)	0.000	0.002	0.115	0.002	0.628	0.05
	AC33	0.958	0.845	44.50 (66)	0.981	0.05	0.396	0.002	0.100	0.002
Linnet Reef	AC37	0.783	0.891	105.3 (105)	0.475	0.006	0.278	0.001	0.26	0.004
	AC42	0.522	0.940	381.7 (253)	0.000	0.001	0.128	0.001	0.567	0.025
	AC33	0.739	0.713	61.71 (21)	0.000	0.001	0.439	0.002	0.119	0.002
Martin Reef	AC37	0.792	0.833	48.66 (55)	0.714	0.01	0.325	0.002	0.139	0.002
	AC42	0.792	0.944	317.0 (276)	0.045	0.003	0.086	0.002	0.468	0.013
	AC33	0.458	0.703	38.12 (21)	0.012	0.002	0.488	0.002	0.070	0.002
Myrmidon Reef	AC37	0.826	0.870	109.5 (66)	0.001	0.002	0.139	0.002	0.375	0.006
	AC42	0.870	0.862	186.7 (136)	0.003	0.002	0.163	0.002	0.003	0.001
	AC33	0.435	0.580	54.24 (15)	0.000	0.001	0.296	0.002	0.030	0.002
Pith Reef	AC37	0.571	0.715	94.662 (55)	0.001	0.001	0.062	0.003	0.003	0.001
	AC42	0.905	0.934	249.760 (231)	0.189	0.003	0.33	0.004	0.31	0.004
	AC33	0.286	0.323	1.340 (6)	0.696	0.03	0.173	0.004	0.02	0.001

Table 2: Continued

Location	Locus	H _O	H _E	Heterozygote excess			IAM		SMM	
				λ^2 (df)	P	α	P	α	P	α
Trunk Reef	AC37	0.333	0.700	53.850 (21)	0.000	0.001	0.329	0.008	0.048	0.002
	AC42	1.000	0.920	177.000 (153)	0.090	0.003	0.466	0.01	0.211	0.003
	AC33	0.4	0.429	16.116 (6)	0.013	0.002	0.266	0.01	0.056	0.002
Britomart Reef	AC37	0.833	0.851	74.258 (55)	0.043	0.003	0.177	0.001	0.313	0.005
	AC42	0.917	0.943	253.667 (253)	0.476	0.007	0.056	0.001	0.34	0.005
	AC33	0.292	0.369	24.026 (3)	0.000	0.001	0.494	0.001	0.214	0.003
Orpheus Island	AC37	0.870	0.854	38.671 (55)	0.953	0.02	0.155	0.002	0.359	0.006
	AC42	0.826	0.911	205.949 (171)	0.035	0.003	0.454	0.003	0.102	0.002
	AC33	0.217	0.553	85.458 (36)	0.000	0.001	0.037	0.003	0.000	0.001
Polmaise Reef	AC37	0.769	0.698	23.111 (21)	0.338	0.004	0.294	0.004	0.049	0.002
	AC42	0.692	0.787	76.349 (45)	0.002	0.002	0.163	0.005	0.019	0.001
	AC33	0.154	0.500	9.030 (3)	0.029	0.002	0.366	0.005	0.419	0.008
Broomefield Reef	AC37	0.917	0.845	44.499 (45)	0.493	0.008	0.109	0.001	0.451	0.01
	AC42	0.708	0.799	56.154 (36)	0.017	0.002	0.311	0.001	0.185	0.003
	AC33	0.042	0.376	48.018 (6)	0.000	0.001	0.261	0.001	0.037	0.002
One Tree Island	AC37	0.722	0.832	50.604 (45)	0.262	0.004	0.314	0.003	0.199	0.003
	AC42	0.833	0.926	251.520 (190)	0.002	0.002	0.537	0.003	0.182	0.002
	AC33	0.500	0.637	22.926 (21)	0.348	0.005	0.208	0.003	0.01	0.001
Sykes Reef	AC37	0.774	0.770	48.331 (45)	0.341	0.004	0.464	0.006	0.023	0.002
	AC42	0.806	0.922	275.629 (210)	0.002	0.002	0.204	0.006	0.216	0.003
	AC33	0.290	0.674	134.038 (45)	0.000	0.001	0.127	0.007	0.003	0.001

Table 3: Analysis of Molecular Variance based on a) mtDNA control region, b) the Infinite Allele Model (IAM) and c) the Stepwise Mutation Model (SMM) of three microsatellite loci among three regions (North, Central and South) of *Acanthochromis polyacanthus* on the Great Barrier Reef. V = Variance component, % = percent variation explained, fixation = fixation index (mtDNA = Φ_{ST} , IAM = F_{ST} and SMM = R_{ST}) and P = significance.

	Among regions				Among populations within regions				Within populations			
	V	%	Fixation	P	V	%	Fixation	P	V	%	Fixation	P
a) mtDNA	17.99	81.21	0.812	<0.0001	1.93	8.71	0.463	<0.0001	2.23	10.0.8	0.90	<0.0001
b) IAM	0.101	7.24	0.072	<0.0001	0.104	7.51	0.081	<0.0001	1.183	85.26	0.147	<0.0001
c) SMM	189.7	19.45	0.195	<0.0001	99.95	10.24	0.127	<0.0001	685.9	70.31	0.297	<0.0001

Table 4: Analysis of Molecular Variance, fixation indices and significance based on a) mtDNA control region, b) the Infinite Allele Model (IAM) and c) the Stepwise Mutation Model (SMM) of three microsatellite loci among inner, mid and outer shelf locations in the northern and central regions of the Great Barrier Reef. V = Variance component, % = percent variation explained, fixation = fixation index (mtDNA = Φ_{ST} , IAM = F_{ST} and SMM = R_{ST}) and P = significance.

	Among shelves				Among populations within shelves				Within populations			
	V	%	Fixation	P	V	%	Fixation	P	V	%	Fixation	P
a) mtDNA:												
Northern	2.677	31.10	0.311	<0.001	1.625	18.87	0.274	<0.001	4.307	50.03	0.450	<0.001
Central	0.127	9.68	0.097	0.169	0.442	33.72	0.373	<0.001	0.742	56.60	0.434	<0.001
b) IAM:												
Northern	0.059	4.320	0.043	0.063	0.034	2.500	0.026	<0.001	1.268	93.18	0.068	<0.001
Central	0.113	8.860	0.089	0.064	0.049	3.820	0.042	<0.001	1.114	87.32	0.127	<0.001
c) SMM:												
Northern	36.36	3.630	0.036	0.138	107.3	10.73	0.111	<0.001	857.1	85.64	0.144	<0.001
Central	81.89	11.28	0.113	0.015	4.857	0.67	0.008	0.376	639.1	88.05	0.120	<0.001

Pairwise genetic distances among populations differed among markers and mutational models (Table 5) but were similar among regions (Table 6). Φ_{ST} values were significantly greater than 0 in more than 97% of all pairwise comparisons. Nuclear pairwise genetic distances were generally less than half those estimated by mtDNA and were statistically significant in 72% of comparisons (83.2% before Bonferroni correction) although this varied between mutational models (significant comparisons $R_{ST} = 52\%$ (71.4% before Bonferroni correction), $F_{ST} = 91.5\%$ (97.1% before Bonferroni correction)). There was no consistent geographical pattern in the variation between models with F_{ST} indicating higher fixation in 37.3, 53.3 and 68% of northern, central and southern comparisons than comparable R_{ST} estimates. (Table 5).

Results of the isolation-by-distance analyses were largely congruent with those of the AMOVAs. Significant correlations between geographical and genetic distance were only evident at the largest spatial scale, i.e. among regions (Φ_{ST} vs. km: $r = 0.77$ $P = 0.001$; F_{ST} vs. km: $r = 0.46$ $P = 0.001$; R_{ST} vs. km: $r = 0.53$ $P = 0.002$ Fig. 2). Genetic and geographic distances did not correlate within regions using any of the genetic markers or distance measures ($P > 0.05$ in all cases, unpublished data).

The metapopulation propagule-pool model was supported in all three regions (Table 7). Fixation indices were higher among younger populations compared to older ones in all regions when based on mtDNA (Table 7). Fixation indices based on both microsatellite models were higher among younger populations in the central region, but not in the northern or southern regions. In both these regions, a large proportion of the pairwise genetic distances based on microsatellites were not significantly different from 0 and this lack of genetic structure may have affected this comparison.

There was substantial variation in migration rates among populations, regions and markers (Fig. 3). Migration rates based on mtDNA were generally low ($4N_eM$ mostly < 1) and reciprocal rates (i.e., $4N_eM$ (a to b) vs. $4N_eM$ (b to a)) were significantly different in 26.7 % of northern, 40% of central and 66.7% of southern pairwise comparisons (Fig. 3). Migration rates based on microsatellites were generally higher (mostly ranging from 1 – 4) and significant reciprocal pairwise differences were less common (North = 6.7%, Central = 10% and South = 16.7%).

Table 5: Pairwise genetic distances among all sampling locations. Pairwise Φ_{ST} estimates are presented above the diagonal, and F_{ST} and R_{ST} estimates are presented below it. Location abbreviations follow Table 1.

		DAY	YON	LIZ	NDR	LIN	MAR	MYR	PIT	TRU	BRI	ORP	OTI	SYK	POL	BRO
		Φ_{ST}														
DAY		x	0.146	0.053	0.487	0.414	0.814	0.574	0.507	0.612	0.552	0.587	0.957	0.947	0.941	0.949
			*	ns	**	**	**	**	**	**	**	**	**	**	**	**
		x														
YON	F_{ST}	0.042	x	0.14	0.545	0.482	0.863	0.655	0.561	0.707	0.621	0.622	0.977	0.971	0.966	0.971
		ns		*	**	**	**	**	**	**	**	**	**	**	**	**
	R_{ST}	0.345	x													
		**														
LIZ	F_{ST}	0.062	0.096	x	0.263	0.201	0.65	0.407	0.344	0.427	0.373	0.403	0.913	0.895	0.886	0.901
		**	**		*	*	**	**	**	**	**	**	**	**	**	**
	R_{ST}	0.267	0.134	x												
		**	ns													
NDR	F_{ST}	0.067	0.098	0.011	x	0.034	0.214	0.592	0.559	0.594	0.579	0.579	0.882	0.858	0.847	0.867
		**	**	ns		ns	**	**	**	**	**	**	**	**	**	**
	R_{ST}	0.308	0.213	-0.014	x											
		**	**	ns												

Table 5: Continued

		DAY	YON	LIZ	NDR	LIN	MAR	MYR	PIT	TRU	BRI	ORP	OTI	SYK	POL	BRO
		Φ_{ST}	Φ_{ST}	Φ_{ST}	Φ_{ST}	Φ_{ST}	Φ_{ST}	Φ_{ST}	Φ_{ST}	Φ_{ST}	Φ_{ST}	Φ_{ST}	Φ_{ST}	Φ_{ST}	Φ_{ST}	Φ_{ST}
LIN	F _{ST}	0.041 **	0.072 **	0.084 **	0.081 **	x	0.33 **	0.541 **	0.508 **	0.544 **	0.528 **	0.544 **	0.882 **	0.859 **	0.849 **	0.868 **
	R _{ST}	0.156 ns	0.027 ns	0.069 ns	0.127 ns	x										
MAR	F _{ST}	0.021 ns	0.053 *	0.074 **	0.078 **	0.024 ns	x ns	0.88 **	0.862 **	0.889 **	0.881 **	0.884 **	0.954 **	0.943 **	0.935 **	0.944 **
	R _{ST}	0.141 ns	0.053 ns	0.081 ns	0.134 ns	-0.018 ns	x ns									
MYR	F _{ST}	0.087 **	0.142 **	0.122 **	0.122 **	0.057 **	0.077 **	x **	0.357 **	0.616 **	0.406 **	0.584 **	0.987 **	0.982 **	0.977 **	0.981 **
	R _{ST}	0.323 **	0.007 ns	0.08 ns	0.149 **	0.0 ns	0.015 ns	x ns								
PIT	F _{ST}	0.137 **	0.186 **	0.191 **	0.197 **	0.119 **	0.093 **	0.066 **	x **	0.255 **	0.053 ns	0.384 **	0.98 **	0.975 **	0.97 **	0.975 **
	R _{ST}	0.429 **	0.009 ns	0.185 **	0.262 **	0.04 ns	0.056 ns	0.009 ns	x ns							
TRU	F _{ST}	0.118 **	0.168 **	0.18 **	0.173 **	0.101 **	0.079 **	0.079 **	0.019 ns	x **	0.352 **	0.689 **	0.993 **	0.989 **	0.983 **	0.987 **

Table 5: Continued

		DAY	YON	LIZ	NDR	LIN	MAR	MYR	PIT	TRU	BRI	ORP	OTI	SYK	POL	BRO
		Φ_{ST}	Φ_{ST}	Φ_{ST}	Φ_{ST}	Φ_{ST}	Φ_{ST}	Φ_{ST}	Φ_{ST}	Φ_{ST}	Φ_{ST}	Φ_{ST}	Φ_{ST}	Φ_{ST}	Φ_{ST}	Φ_{ST}
TRU	R _{ST}	0.321 **	-0.01 ns	0.115 ns	0.188 **	0.001 ns	0.014 ns	-0.017 ns	-0.023 ns	x						
BRI	F _{ST}	0.109 **	0.153 **	0.173 **	0.170 **	0.082 **	0.075 **	0.052 **	0.026 ns	0.014 ns	x	0.389 **	0.988 **	0.984 **	0.979 **	0.983 **
	R _{ST}	0.199 **	0.013 ns	0.096 ns	0.166 **	-0.016 ns	-0.004 ns	0.005 ns	0.046 **	0.002 ns	x					
ORP	F _{ST}	0.116 **	0.163 **	0.079 **	0.096 **	0.130 **	0.142 **	0.122 **	0.212 **	0.216 **	0.199 **	x	0.989 **	0.985 **	0.98 **	0.984 **
	R _{ST}	0.589 **	0.158 **	0.209 **	0.263 **	0.236 **	0.267 **	0.196 **	0.214 **	0.185 ns	0.251 **	x				
OTI	F _{ST}	0.109 **	0.148 **	0.06 **	0.069 **	0.126 **	0.133 **	0.135 **	0.22 **	0.211 **	0.198 **	0.062 **	x	0.459 **	0.085 *	0.59 **
	R _{ST}	0.595 **	0.235 ns	0.281 **	0.33 **	0.309 ns	0.335 **	0.282 **	0.273 **	0.244 ns	0.325 **	0.037 ns	x			
SYK	F _{ST}	0.136 **	0.179 **	0.099 **	0.144 **	0.136 **	0.158 **	0.132 **	0.218 **	0.227 **	0.205 **	0.049 **	0.021 ns	x	0.15 *	0.099 *

Table 5: Continued

		DAY	YON	LIZ	NDR	LIN	MAR	MYR	PIT	TRU	BRI	ORP	OTI	SYK	POL	BRO
		Φ_{ST}														
SYK	R _{ST}	0.76	0.437	0.489	0.521	0.494	0.518	0.502	0.516	0.479	0.519	0.172	-0.007	x		
		**	**	**	**	**	**	**	**	**	**	**	**	ns		
POL	F _{ST}	0.182	0.222	0.136	0.119	0.186	0.192	0.189	0.276	0.268	0.241	0.108	0.107	0.141	x	0.297
		**	**	**	**	**	**	**	**	**	**	**	**	**	**	
BRO	R _{ST}	0.516	0.116	0.097	0.134	0.144	0.166	0.10	0.144	0.107	0.172	0.017	0.095	0.315	x	
		**	ns	ns	ns	ns	ns	**								
BRO	F _{ST}	0.175	0.212	0.099	0.107	0.188	0.192	0.191	0.276	0.277	0.257	0.086	0.057	0.092	0.063	x
		**	**	**	**	**	**	**	**	**	**	**	*	**	ns	
BRO	R _{ST}	0.681	0.255	0.266	0.307	0.293	0.317	0.269	0.307	0.268	0.333	0.022	0.08	0.306	0.01	x
		**	**	**	**	**	**	**	**	**	**	**	ns	ns	**	ns

Significant of comparisons indicated as follows: ** = $P < 0.001$, * = $0.05 < P$, ns = non-significant comparisons (in bold if insignificant following Bonferroni correction)

Table 6: Average genetic differentiation within regions among markers and mutational models

Region	Mean Φ_{ST} (95% CI)	Mean F_{ST} (95% CI)	Mean R_{ST} (95% CI)
North	0.38 (0.13)	0.06 (0.01)	0.13 (0.05)
Central	0.41 (0.11)	0.10 (0.05)	0.09 (0.07)
South	0.28 (0.17)	0.08 (0.03)	0.13 (0.11)

Table 7: Strength of genetic differentiation among older and younger populations. Location abbreviations follow Table 1.

Marker	Older	Younger	Youngest	Support
Northern region	DAY-YON	LIZ-NDR	MAR-LIN	
Φ_{ST}	0.146	0.236	0.33	Yes
F_{ST}	0.042	0.011	0.024	No
R_{ST}	0.345	-0.014	-0.02	No
Central region	PIT-MYR		ORP-TRU	
Φ_{ST}	0.357		0.689	Yes
F_{ST}	0.066		0.216	Yes
R_{ST}	0.009		0.185	Yes
Southern region	POL-BRO		SYK-OTI	
Φ_{ST}	0.297		0.459	Yes
F_{ST}	0.063		0.021	No
R_{ST}	0.01		-0.001	No

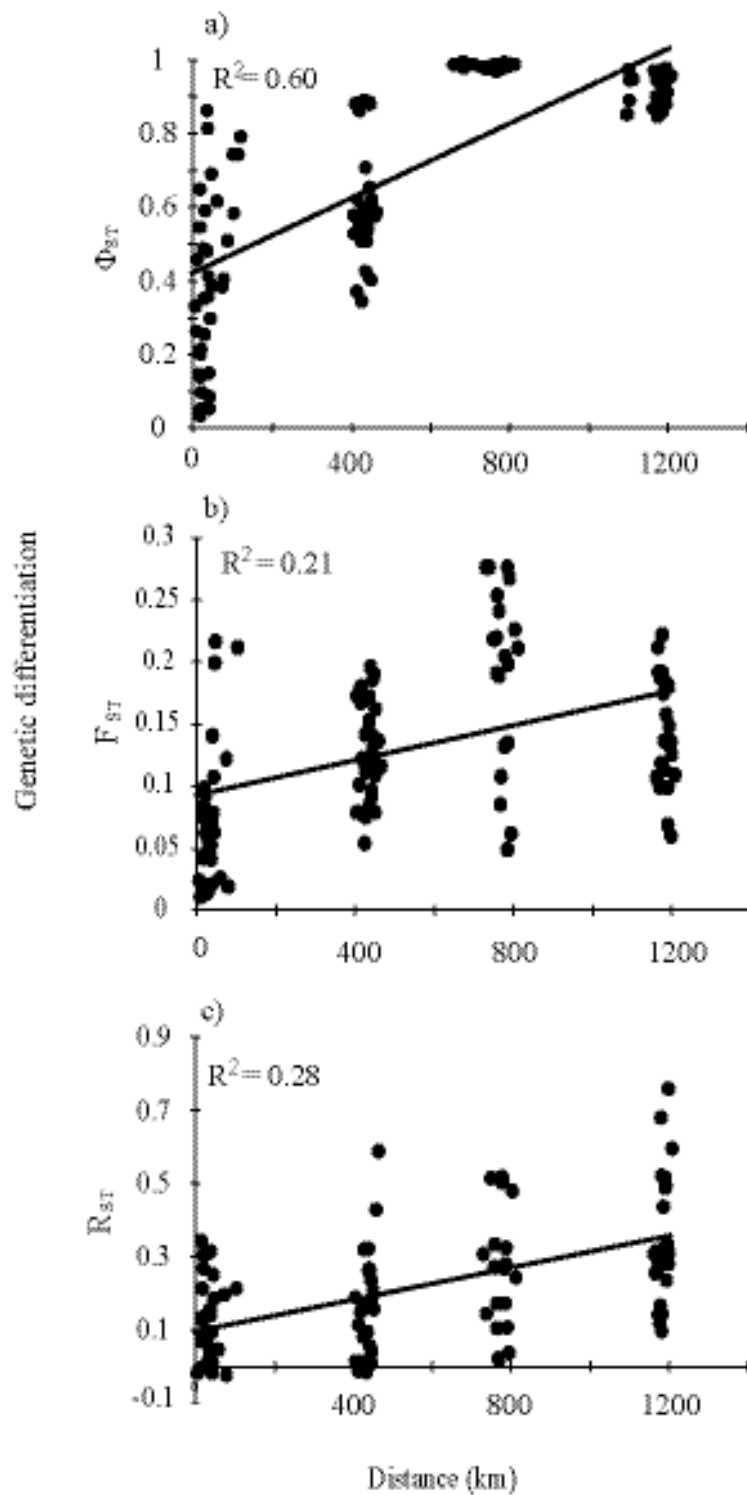


Fig. 2: Relationship between genetic differentiation and linear distance based on a) mtDNA ($\Phi_{ST} = 0.00051 (0.00043 - 0.00058)km + 0.41 (0.36 - 0.47)$ b) microsatellites (IAM) ($F_{ST} = 0.00007 (0.000044 - 0.000096)km + 0.09 (0.07 - 0.11)$) and c) microsatellites (SMM) ($R_{ST} = 0.00022 (0.00015 - 0.00029)km + 0.087 (0.04 - 0.13)$).

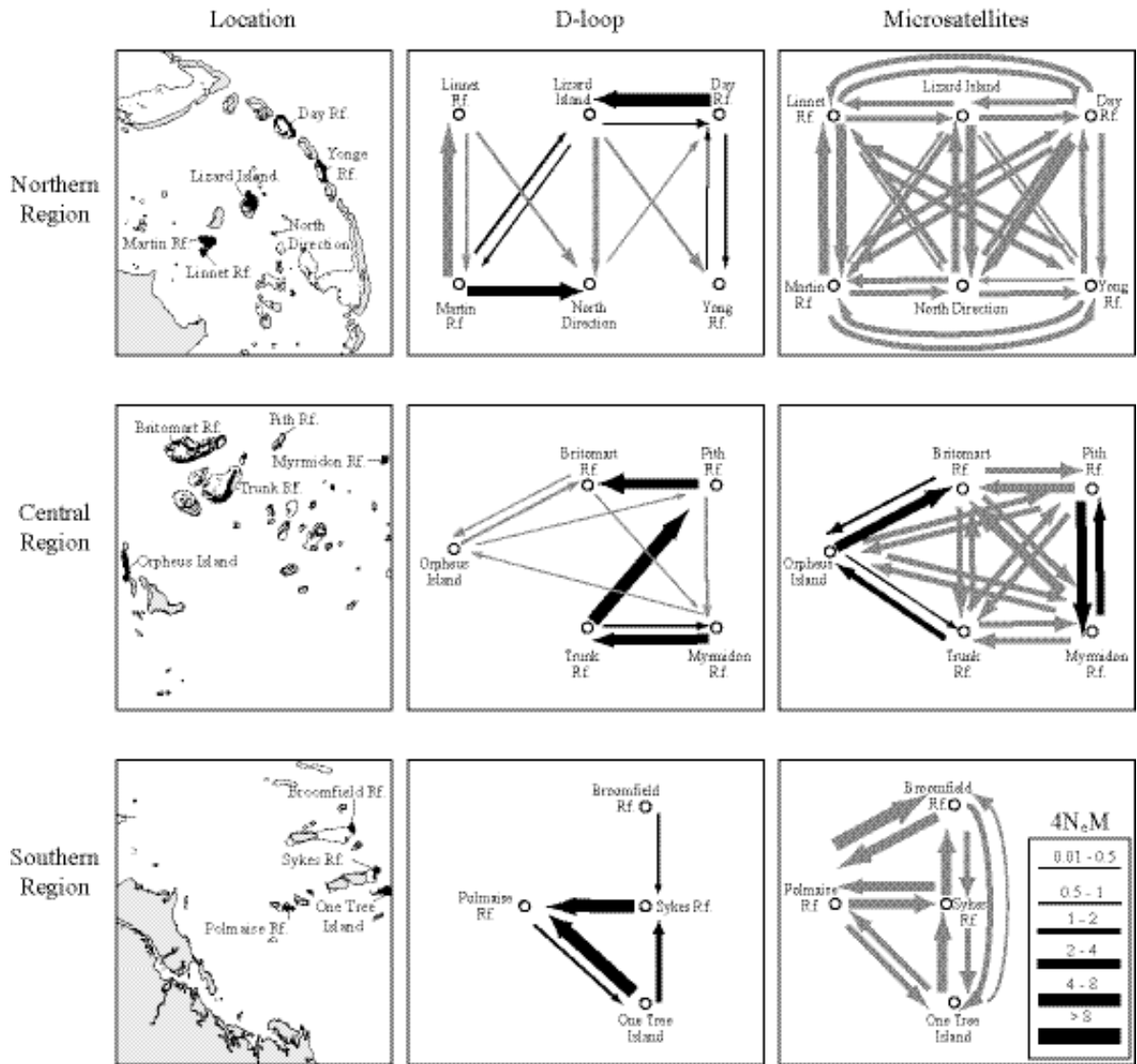


Fig. 3: Reciprocal migration rates ($4N_e m$) among reefs in the northern, central and southern regions estimated for the mtDNA (Control region) and the microsatellites. The thickness of the arrows indicate the migration rates and the colour indicates statistical difference between reciprocal migration rates (black = 95% confidence intervals of estimates did not overlap; grey = 95% confidence intervals of estimates overlapped).

For both markers, the frequency of significantly different migration rates between populations increased in a north – south direction and all regions were characterised by one or two mitochondrial migration rates being significantly higher ($4N_e m \sim 4$) than all other estimates. Migration rates based on mtDNA and microsatellites were significantly different in 80% of northern, 75% of central and 58.3% of southern comparisons (Fig. 3). The microsatellites consistently indicated higher migration rates (north: 91.6%, central: 93.3 %, south: 71.4%) compared to those estimated based on mtDNA, although

higher mtDNA migration rates were occasionally found (north: 8.3%, central: 6.7%, south: 28.8%).

Reductions in microsatellite sample sizes by one third and one sixth, to make them comparable to the sample size used for the mtDNA (i.e., one marker, one haploid marker) did not substantially affect estimates of migration (although variances increased as expected) (Appendix 1). When significant differences occurred there was no consistent pattern in which data set indicated higher or lower migration rates (Appendix 1).

Discussion

This study revealed strong genetic structure among populations of *A. polyacanthus* on the GBR. There were substantial differences in the spatial structure and migration rates within and among regions and molecular markers. This suggests that the genetic structure of this species is complex and that understanding the evolution of the structure revealed here will require knowledge of the operation of processes operating in a scale-dependent fashion.

Genetic structure among regions

Strong genetic structure among northern, central and southern regions of the GBR was revealed by analyses of both mtDNA and nuclear markers. This pattern conforms to previous findings for this species of strong structure between northern and southern regions based on allozyme markers (Doherty et al. 1994; Planes et al. 2001) and indicates the presence of further strong structuring among bi-coloured morphs between northern and central locations. My analyses of both mitochondrial and nuclear markers indicated that this structure followed an isolation-by-distance model of dispersal where genetic exchange is more likely among neighbouring locations (Fig. 2). Consequently, at this spatial scale, *A. polyacanthus* does not appear to function as a metapopulation. While patterns of isolation-by-distance have been reported at large spatial scales in marine organisms (e.g., Palumbi et al. 1997; Planes and Fauvelot 2002) this study reports one of very few examples of such dynamics across small spatial scales (see also Planes et al. 1996). The relationships between geographical and genetic distances among these populations varied within and among markers, but in general, the within population divergence (i.e., intercepts) estimated by the IAM and SMM models were similar, and less than that estimated from mtDNA. Genetic divergence accumulated

more quickly with distance (i.e., slopes) when estimated using the mtDNA compared to microsatellites (Fig. 2). This difference would be expected given the slower fixation rates of co-dominant compared to haploid markers and indicates that this may be occurring here (see below).

Genetic structure within regions

Strong genetic structuring was revealed within all three regions (Table 5). This variation was attributable to shelf position for the mtDNA marker in the northern region and for the microsatellite data under the SMM model in the central region (Table 4). No evidence of isolation-by-distance was found within either the northern or the central region. Therefore, although initial colonisation of the continental shelf may have occurred from the outer to inner continental shelf in the northern and central regions, other processes have erased any signature of this process in these genetic markers. Genetic differentiation among populations within regions was similar among regions (Table 6) and generally very high particularly in the mtDNA analyses (Table 5). For example, Lizard Island (LIZ) and North Direction Island (NDR) are separated by less than 10 km but have a Φ_{ST} value of 0.26 and Martin Reef (MAR) and Linnet Reef (LIN) are separated by less than 6 km and have a Φ_{ST} value of 0.33. Such differentiation is among the highest recorded for any coral reef fish at such small spatial scales (e.g., Doherty et al. 1995; Dudgeon et al. 2000; Chapter 5) and is comparable to values obtained in other studies of direct-developing reef fishes at similar spatial scales (Bernardi 2000; Bernardi and Vagelli 2004; Hoffman et al. 2005; van Herwerden and Doherty 2006). This finding suggests that the spatial patterns described by this study may be broadly applicable to direct developing reef fish species.

The propagule-pool model was supported in all comparisons dominated by pairwise fixation indices significantly greater than 0 (Table 7). The strength of fixation indices increased from older to younger populations in these comparisons, however, sample sizes did not permit statistical testing of these results (Table 7). These results add to only a handful of empirical investigations that have explored the predictions of these models (reviewed by Giles and Goudet 1997). The majority of these previous investigations reported that younger populations displayed greater genetic differentiation than older ones (but see Dybdahl 1994) which is congruent with the results of this study.

Asymmetric migration rates

There were considerable asymmetries in migration rates among locations based on mtDNA data. All regions were characterised by high frequencies of significantly different reciprocal migration rates and one or two migration rates that were much greater than the rest (Fig. 3). Insignificant pairwise Φ_{ST} values (based on mtDNA) were often (e.g., Day – Lizard Island; Britomart – Pith) but not always (e.g. North Direction – Linnnet) associated with significantly asymmetric migration rates. Conversely, higher and asymmetric migration rates were occasionally detected between locations with low but significant genetic structuring (e.g., North Direction – Martin; One Tree Island – Polmaise; Sykes - Polmaise). Consequently, migration rates based on mtDNA data were complex and gene flow occurred, although generally at low rates, both uni- and bi-directionally among the sampled locations. Examples of asymmetric migration rates based on genetic evidence are emerging (e.g., Fraser et al. 2004) and emphasise the potential role of such variation in the dynamics of metapopulations (Hanski and Gilpin 1997; Stacey et al. 1997). In contrast, migration rates based on the microsatellites were generally high, mostly symmetrical and uniform among locations. There were no clear differences in migration rates between locations with significant genetic structure compared to those without. These results suggest that migration patterns may be sex-biased (discussed below).

Differences among markers

In general, patterns of lower genetic differentiation and higher migration rates among populations, shelf position and regions were estimated for nuclear as compared to mtDNA markers. Such differences in estimates of fixation may arise due to differences in the levels of heterozygosity between markers (Hedrick 1999, 2005). In addition at least another three processes may have contributed to this difference between the results obtained with these two different classes of markers.

Differences in migration rates and genetic structure between markers may have been due to the larger sample sizes of the microsatellites (3 loci, 2 alleles per locus) compared to the mtDNA (1 allele, 1 locus). However, substantial reduction of the microsatellite sample size did not materially change the migration rates estimated from them (although variances did increase substantially) (Appendix 1). It is, therefore, unlikely that these observed differences were due to sampling issues alone.

Slower fixation rates of neutral nuclear markers compared to mitochondrial ones because of greater effective population sizes (Birky et al. 1989; Neigel 1997, 2002; Balloux et al. 2000) may have contributed to the patterns observed here. This difference in fixation rates may also explain the pattern of pairwise genetic distances in the northern region where there was a westward trend of decreasing difference coinciding with the presumed age of the populations. Consequently, slower fixation of nuclear markers may have affected estimates of migration. The significant structure found by the microsatellites in a large proportion of the comparisons (75%), however, indicates that other processes may also be operating. It is also possible that the low number of loci, high heterozygosity and moderate sample sizes did not permit accurate estimation of the population genetic structure. If so, genetic differentiation estimates from all populations should be equally affected (assuming equal N_e and genetic diversity among populations). Levels of genetic structure varied greatly, from very high to very low, among populations separated by approximately equal distances. It is, therefore, unlikely that differences in fixation rates alone were responsible for the observed pattern.

The third possibility is that the higher migration rates estimated based on microsatellites compared to mtDNA is the results of male-biased dispersal. Sex-biased dispersal may evolve where there are differential fitness consequences with respect to sex associated with acquiring and defending reproductive resources such as territorial space (e.g., Greenwood 1980; Clarke et al. 1997). Dispersal tends to be female biased in birds (Greenwood 1980) and male biased in mammals (Dobson 1982) and fishes (Hutchings and Gerber 2002; Fraser et al. 2004). Differences in pairwise genetic differentiation and migration rates observed here suggest that male-biased dispersal is occurring in this species. If so, this study provides the first documented example of sex-biased dispersal in coral-reef fishes. However, until the effects of male-biased dispersal and slower fixation of microsatellites can be separated unequivocally some uncertainty of this interpretation remains.

Differences among mutational models

Pairwise genetic estimates of R_{ST} and F_{ST} among populations differed greatly (Table 5) despite apparent conformity of the data with the assumptions of both models (Table 2). While it is not always possible to evaluate which statistic provides a better estimate (Balloux and Goudet 2002), R_{ST} calculations incorporate more biologically realistic assumptions by taking into account the evolutionary relationships among alleles (Estoup

and Cornuet 1999), and may provide better estimates when mutation contributes significantly to allelic differences between populations (Goldstein et al. 1995; Pérez-Lezaun et al. 1997). R_{ST} estimates, however, may also be associated with greater variances, especially if analyses are based on a low number of loci (Nei 1995; Takezaki and Nei 1996; Neigel 2002). In contrast, F_{ST} may provide a potentially biased estimate (because the effects of migration and mutation cannot be separated) but are typically associated with less error (Balloux and Goudet 2002). My results are consistent with these patterns; F_{ST} estimates were generally smaller but less variable than R_{ST} estimates (Table 5). While an extensive analysis of which mutational model better describes the data is beyond the objectives of the current study, the high mutation rates of microsatellites may have affected estimated levels of fixation here and ‘true’ fixation levels are probably somewhere between those estimated by both models, that is, low but in many instances significantly greater than zero.

Conclusion

The population genetic structure of *A. polyacanthus* on the GBR contained significant scale-dependent variation consistent with isolation-by-distance and metapopulation models. Within regions, there was high levels of population structure and low and asymmetric migration. While the population structure of *A. polyacanthus* on the GBR strongly suggests that this species displays metapopulation dynamics, a crucial distinction between such a genetic system and others including island (Wright 1931) and patchy population models (Harrison 1991; Planes et al. 1996) lie in the occurrence and frequency of local extinctions. I examine the evidence for population bottlenecks and extinctions in a subsequent investigation of the genetic structure of this species (Chapter 3).